Ann. Geophys., 26, 2459–2470, 2008
www.ann-geophys.net/26/2459/2008/

Annales Geophysicae

Lower E-region echoes over the magnetic equator as observed by the MF radar at Tirunelveli (8.7° N, 77.8° E) and their relationship to E_{sq} and E_{sb}

R. Dhanya, S. Gurubaran, and K. Emperumal

Equatorial Geophysical Research Laboratory, Indian Institute of Geomagnetism, Krishnapuram, Tirunelveli 627 011, India

Received: 7 November 2007 – Revised: 24 June 2008 – Accepted: 7 July 2008 – Published: 15 August 2008

Abstract. The spaced antenna medium frequency (MF) radar at Tirunelveli (8.7° N, 77.8° E, geographic; 1.7° N, magnetic dip), the only one of its kind currently operating close to the magnetic equator, has provided an opportunity to investigate the electrodynamical processes related to the equatorial electrojet (EEJ) and their influence on the radar scatterers at medium frequencies in the lower E-region heights (90–98 km). Making use of the full correlation analysis that enables determination of useful geometrical parameters from the ground diffraction pattern, the present work delineates for the first time the characteristics of the radar scatterers during the occurrences of equatorial sporadic E (E_{sq}) and blanketing sporadic E (E_{sb}) noticed in simultaneous ionospheric sounding records at Tirunelveli. The ground magnetometer data provide indirect information on the strength of the EEJ and afternoon reverse EEJ or counterelectrojet (CEJ). The results presented in this work also reveal the height dependence of the radar echo intensity and some of the geometrical parameters at certain times, thus clearly bringing out the complex interplay of various physical processes in the probing region.

Keywords. Ionosphere (Equatorial ionosphere; Ionospheric irregularities; Plasma waves and instabilities) – Radio science (Ionospheric physics)

1 Introduction

The partial reflection drift (PRD) technique has been yielding reliable estimates of upper mesospheric winds for more than three decades. Despite the limitations common for any radar technique, spaced antenna MF radar wind measurements provide useful information on mean winds, planetary-scale waves, tides and gravity waves in the mesosphere-lower thermosphere (MLT) region (Vincent, 1984). The MF radar operating at Tirunelveli has been providing useful data for more than a decade on mean winds, tides and planetary waves. Previous work using data from this site clearly revealed that the MF radar echoes at 90 km and above are influenced by electrodynamical processes (Gurubaran and Rajaram, 2000; Ramkumar et al., 2002; Gurubaran et al., 2007). For radar systems operating in the vicinity of the magnetic equator, complexities in interpreting the drift measurements in terms of neutral winds arise due to the presence of the equatorial electrojet (EEJ) that plays a dominant role in the generation and movement of electron density irregularities in the lower E region (Kelley, 1989).

The EEJ is believed to be a seat of a variety of plasma instabilities driven by the ambient zonal and vertical electric fields and background density gradient of various scale sizes. An understanding of the physics underlying these instabilities has come from VHF/HF radar observations (Fejer et al., 1975; Crochet et al., 1979; Reddy et al., 1987; Tsunoda and Ecklund, 1999; Abdu et al., 2002; Devasia et al., 2004). The two-stream plasma instability gives rise to Type-I irregularities in plasma during the times of strong electrojet currents accompanied by large electron drift velocities (Farley, 1963). The gradient drift instability or cross-field instability is generated when vertical electron density gradient in electrojet plasma is perpendicular to electrojet current and gives rise to Type-II irregularities (Farley and Balsley, 1973).

A phenomenon related to EEJ is the equatorial sporadic E, commonly referred to as E_{sq}, which is a manifestation of Type-II echoes (Balsley et al., 1976). When the EEJ reverses or during the counterelectrojet (CEJ) conditions, the Type-II echoes as recorded in a VHF radar disappear because of the weakening or even reversal of the ambient eastward electric field (Fejer et al., 1976). Rastogi (1972) showed that E_{sq} occurs at an altitude of maximum gradient in electron density in the presence of a Hall polarization field and suggested that E_{sq} observed in an ionogram is due to the scattering of

Correspondence to: R. Dhanya
(dhanya.ramani@gmail.com)

Published by Copernicus Publications on behalf of the European Geosciences Union.

radio waves by the irregularities generated due to gradient drift instability. It was subsequently shown that E_{sq} disappears during a CEJ event (Rastogi, 1973).

The other type of anomalous ionospheric reflection as evidenced in the ground ionograms from an equatorial station is the blanketing sporadic E (E_{sb}) which occurs mostly during late afternoon hours and in local summer months (Chandra and Rastogi, 1975). It is well established E_{sq} occurs during periods of strong electrojet, while E_{sb} occurs during weak or reversed electrojet (Chandra and Rastogi, 1974). The occurrence of E_{sb} is attributed to overdense reflection from thin layers of enhanced ionization that effectively blanket the upper ionosphere from the probing ionospheric sounding frequencies. Blanketing occurs during a weak EEJ or CEJ, most often the latter. On certain occasions, CEJ can be considered as a seat of both Type-I and Type-II irregularities, just as the daytime electrojet is a seat of both Type-I and Type-II irregularities (Devasia et al., 2004).

The scattering or reflection processes responsible for the MF radar echoes at heights above 90 km considered in this work are expected to respond to the changing electrodynamical conditions depending on the local time. Spaced receiver techniques at HF frequencies were used in the past to detect the plasma drift motions and decipher the nature of the irregularities responsible for producing fading in the spaced receiver records (Chandra and Rastogi, 1973; Tabbagh et al., 1977). Chandra and Rastogi (1973) noticed that at times of E_{sq}, the records for the frequency of 4.7 MHz at Thumba (8.5° N, 76.9° E) revealed fast fading, westward drift and highly elongated ground diffraction patterns with a small semi-minor axis. On the other hand, when E_{sq} was absent, the fading rates were too small implying slow fading, the drift direction was reversed to the east and the ground diffraction pattern was almost isotropic. The recent reports that made use of the MF radar observations from Tirunelveli were in conformity to the earlier HF spaced receiver findings (Gurubaran and Rajaram, 2000; Ramkumar et al., 2002; Gurubaran et al., 2007).

The motivation for performing these studies lies in our need for understanding how the combined neutral dynamical and plasma instability processes drive the lower E-region scatterers or irregularities that are responsible for the observed MF radar echoes. Below 90 km, it is anticipated that neutral dynamics involving wave processes contributes to the generation of the radar scatterers, whereas above 90 km we expect plasma instability processes to partly account for the radar echoes and measured drifts. Ramkumar et al. (2002) examined the MF radar observations on day-to-day basis and found the daytime wind and tidal characteristics to exhibit complex behaviour. On certain days, the dynamical parameters revealed close connection to EEJ, whereas on certain other days the drifts at 98 km were different from those expected to be of EEJ origin. These peculiarities in observed drift motions were also noticed in the later work by Gurubaran et al. (2007). Systematic investigations with co-located experiments like digital ionosonde and coherent VHF backscatter radar would provide various clues to understanding the complexities in the MF radar observations made at the magnetic equator. Further, the current understanding of the EEJ irregularities and the underlying physics has come from the HF/VHF measurements. Whether MF radar observations have any scope in understanding the equatorial plasma instability processes is yet to be explored.

The present work makes use of the digital ionosonde operating at Tirunelveli for the first time and reports the results from a case study that analyzes the MF radar echoes and spaced antenna geometrical parameters on two selected days marked by distinct electrodynamical conditions. On one of these days, an afternoon CEJ occurred with the disappearance of E_{sq}. A blanketing sporadic-E event occurred in the presence of an afternoon CEJ on the other day. With the co-located ionosonde, it has become possible to associate certain echo characteristics with the appearance or disappearance of E_{sq}. For the first time, the MF radar observations reported herein provide important insights of the drift velocities and derived geometrical parameters during the occurrence of blanketing sporadic E. Another added feature in this work is the examination of these derived parameters at various heights and inference of their height dependence.

2 Observational details

The 1.98 MHz radar operating at Tirunelveli has been yielding data on winds in the MLT region at heights between 68 and 98 km since mid-1992. The radar transmits linearly polarized 4.5 km long pulses and receives the returns at three spaced receiving antennas. The plane of polarization of the transmitted beam corresponds to "O" mode during daytime and "E" mode during nighttime. Two pairs of transmitting dipole antennas are used, with one pair arranged parallel to the geomagnetic north-south direction and the other pair orthogonal to it. Separate inverted-V type dipoles receive the echoes during day (for the "O" mode) and night (for the "E" mode).

The full correlation analysis (Briggs, 1984) is used to determine dynamical and several spaced antenna parameters. Every estimate obtained from this analysis at a time resolution of around 2 min is based on a 256-sample set, wherein each sample is a result of coherent integration of a predetermined number of pulses. For the radar operating at 50 Hz pulse repetition frequency (PRF), the analysis is performed with 32 coherent integrations during daytime, yielding a time resolution of 0.64 s for each of the 256 samples and around 2.8 min for every wind estimate. During nighttime, the number of coherent integrations is halved and at the same PRF, wind estimates are obtained at 1.4 min time interval. The data analysis that invokes full correlation analysis has several in-built rejection criteria: (1) signal amplitude too low, (2) SNR < -6 dB, (3) fading time > 6 s, (4) at least one cross

correlation function (CCF) maximum lies outside end points, (5) percentage time discrepancy >35%, (6) ground diffraction analysis breaks down, (7) at least one CCF maximum <0.2 and (8) apparent velocity magnitude >400 ms^{-1} or true velocity magnitude >200 ms^{-1}, to name a few. The analysis produces 19 error codes corresponding to each of the rejection criteria. By examining the error codes, it can be ascertained what criterion out of the 19 contributed to the rejection of the data, whenever it happens.

Besides horizontal velocities, the full correlation analysis enables determination of several geometrical parameters corresponding to the ground diffraction pattern for a given acquisition of the data. Useful information on the scatterers can be obtained by examining the geometrical parameters, namely, the pattern lifetime, pattern scale, axial ratio and pattern elongation. The pattern life time has the effects of the mean wind removed and hence represents random changes of the scattering echoes alone. It depends primarily on the atmospheric turbulence below 90 km and on electrodynamical conditions prevailing in the EEJ region above that height. This parameter can therefore be used to infer the stability of the reflecting medium (Lesicar, 1993). The pattern scale is a measure of the extent of the irregularities defining the diffraction pattern. Larger the pattern scale, greater is the extent of the semi-major axis of the ground diffraction pattern, and leads to elongation in a preferable direction. The smaller pattern scale indicates isotropic nature of the scatterers (Lesicar, 1993). The axial ratio is the ratio of semi-major to semi-minor axes of the characteristic ellipse. The pattern elongation renders information about the orientation of the pattern referenced to the geomagnetic north.

This work probes the linkage of MF radar echoes with EEJ with supporting data available from the co-located magnetometer and the vertical incidence ionosonde. Because the radar is operated close to the magnetic equator, the echoes from the lower E-region heights are presumed to be related to the EEJ. The work examines potential underlying mechanisms that influence the geometrical parameters and their relation to electrodynamical processes, in order to get more insights of the nature of the scatterers under varying geophysical conditions.

The 20-min average of the horizontal component of the geomagnetic field variations (ΔH) from the co-located digital fluxgate magnetometer is made use of in the present work. The N-S field variation (ΔH) recorded on the ground represents the height-integrated current density, which over the magnetic equator corresponds to the intense east-west current of EEJ origin. A digital ionosonde has been operating from Tirunelveli since June 2006. We make use of the ionograms available from this site in order to track the appearance and disappearance of E_{sq} at the time resolution of five minutes for the days of interest.

For the present work a few geomagnetically quiet days during June 2007 were identified during which the EEJ conditions were different from one day to the other. Because the overhead current above Tirunelveli is composed of both Sq and EEJ, it is required to eliminate the Sq contribution before we proceed any further. The magnetic field variation at a station outside the electrojet has only the Sq contribution. The difference in ΔH values between the electrojet station, Tirunelveli (TIR) (8.7° N, 77.8° E) and an off-electrojet station, Alibag (ABG) (18.64° N, 72.87° E), is considered, so as to eliminate the Sq and magnetospheric currents, that would lead to the electrojet strength alone. The spaced antenna and the geometrical parameters representing the shape and orientation of ground elliptical diffraction pattern, that were examined on these days, are the signal-to-noise ratio (SNR) representing the intensity of the MF radar echo, the pattern lifetime, the pattern scale size, the axial ratio and the pattern orientation.

We categorized the observations into two cases, both occurring during geomagnetically quiet days: (i) a CEJ day when the E_{sq} disappeared in the afternoon hours (26 June 2007) and (ii) a CEJ day when the E_{sq} disappeared and a blanketing $E_s$event occurred in the afternoon hours (18 June 2007). On the latter day, the E_{sq} was of considerable intensity (10–15 dB greater than the other day) for a brief period in the morning hours.

3 Results

In Fig. 1 we show in contour form the response of the hourly averaged SNR (bottom panels) for receiver 1 in the height region 80–98 km on the two selected days along with the strength of the EEJ [$\Delta H_{\mathrm{TIR}} - \Delta H_{\mathrm{ABG}}$] (top panels). On both these days the SNR values were greater (15–20 dB) at heights above 90 km, primarily due to the EEJ irregularities generated by the primary electric field which is eastward during the normal EEJ conditions. Reduction in SNR values in the afternoon hours at these heights occurred when the EEJ reversed and became westward. It was seen separately in the ionograms that the E_{sq} disappeared when the CEJ conditions prevailed on these days. On 18 June 2007, blanketing E_s was noticed in the ionograms during the afternoon hours. The simultaneous increase in SNR observed at lower E-region heights is attributed to the enhanced ionization layer that is expected to form during a blanketing E_s event. Around 08:00 IST on 18 June 2007, the E_{sq} was of unusually greater intensity and the SNR values at 96 and 98 km clearly show enhancements around this time. An anomalous increase in SNR can be noticed at heights between 86 and 92 km at 17:00 IST after the blanketing E_s disappeared in the ionograms. The hourly averaged SNR plots shown in Fig. 1 portray well the overall behaviour of the MF radar echoes during the varying electrodynamical conditions observed on 18 and 26 June 2007.

In the four-figure sets (Figs. 2a, b, c and d and 3a, b, c and d), we present the results for SNR, the geometrical parameters and the bulk zonal and meridional velocities for the

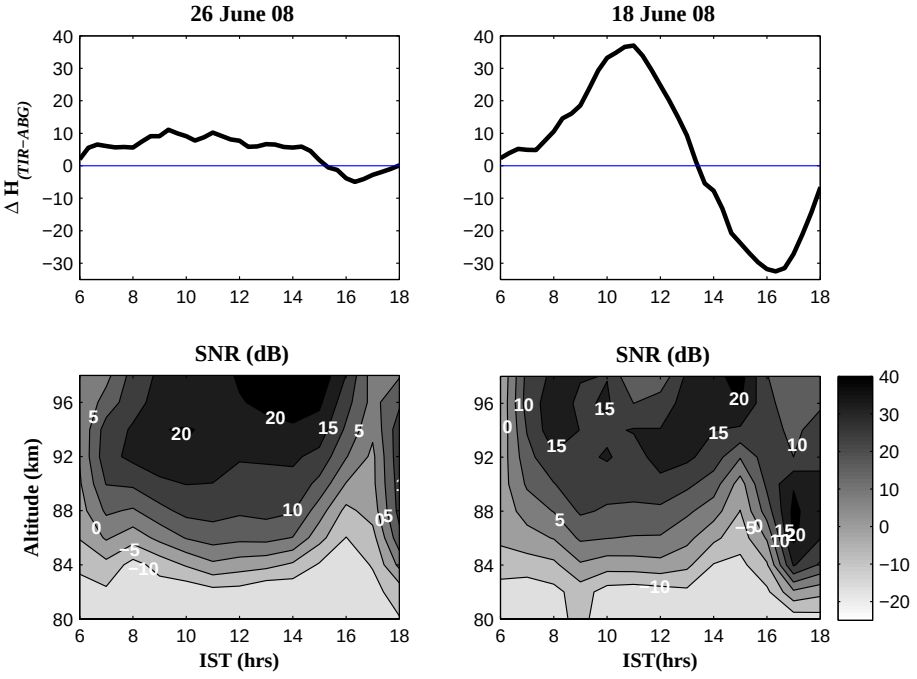

Fig. 1. (top) ΔH determined from the ground magnetometer data from Tirunelveli and Alibag and (bottom) daytime SNR in the height range 80–98 km on 26 June 2007 (left panels) and 18 June 2007 (right panels).

heights 86, 90, 94 and 98 km, determined from the full correlation analysis for the two selected days. In both cases, the top panel of each figure represents the strength of daytime EEJ [$\Delta H_{\mathrm{TIR}} - \Delta H_{\mathrm{ABG}}$]. Figures 2a and 3a depict the SNR (the points correspond to the measurements made at near 2-min time intervals) plotted in the four panels below the EEJ plot. Figures 2b and 3b depict the snapshots of sample ionograms for selected times corresponding to the appearance or disappearance of E_{sq} and appearance of E_{sb}. Figures 2c and 3c show the behavior of geometrical parameters, namely, the pattern life time (s), the pattern scale length (m), the pattern axial ratio and the pattern elongation (angle in degrees marked with reference to geomagnetic north) depicted in the four panels from bottom. The geometrical parameters shown on the left panels are for 86 and 90 km, while those on the right panels are for the heights, 94 and 98 km. The zonal and meridional velocities are plotted in the four panels from the bottom (zonal velocities on the left and meridional velocities on the right) in Figs. 2d and 3d. All specified times are in Indian Standard Time (IST).

Case-I: Quiet CEJ day marked with no E_{sb} (26 June 2007 (A_p=3) (Fig. 2a–d))

This day serves as a clear example for the behavior of MF radar echoes during the times of CEJ without blanketing. The behavior of MF radar scatterers during different phases (growth and decay) of E_{sq} can be studied from this day signified by the absence of E_{sb}. This day is characterized by a weak EEJ followed by partial/weak CEJ as seen in the top panel on the left in Fig. 1. The EEJ magnitude on this day was weak ($\Delta H \approx 11$ nT) compared to the other selected day and so was CEJ ($\Delta H \approx -5$ nT) that commenced at 15:20 IST and lasted till 18:00 IST. The afternoon depression was at its peak at 16:05 IST.

The ionograms showed the presence of E_{sq} from 07:30 IST to 16:00 IST. Two sample ionograms corresponding to times 07:35 IST and 16:05 IST are shown in Fig. 2b. E_{sq} started weakening from the time of ΔH reversal and vanished just before the time the CEJ reached its peak. As can be seen on this day marked by a normal afternoon CEJ without blanketing, the SNR values in the lower E region followed ΔH (refer to Fig. 2a) and the pattern lifetimes at these heights (shown in Fig. 2c) had an inverse relation with ΔH, particularly for the heights 94 and 98 km (refer to the panels on the right in Fig. 2c). During morning hours (08:00 to 10:00 IST), when the EEJ was growing, the pattern lifetimes were around 2 s at 94 and 98 km, whereas in the afternoon hours this parameter was in the range 3–5 s. It is evident from the observations that the SNR increased gradually with E_{sq} and remained high (20–30 dB) till E_{sq} was stronger. The SNR became very small (0–5 dB) when the E_{sq} disappeared. On the other hand, the pattern lifetime was smaller ($\sim$2 s) when E_{sq} was fully developed and remained small till the weakening of E_{sq}, indicating the presence of plasma turbulence and hence randomness of the medium at

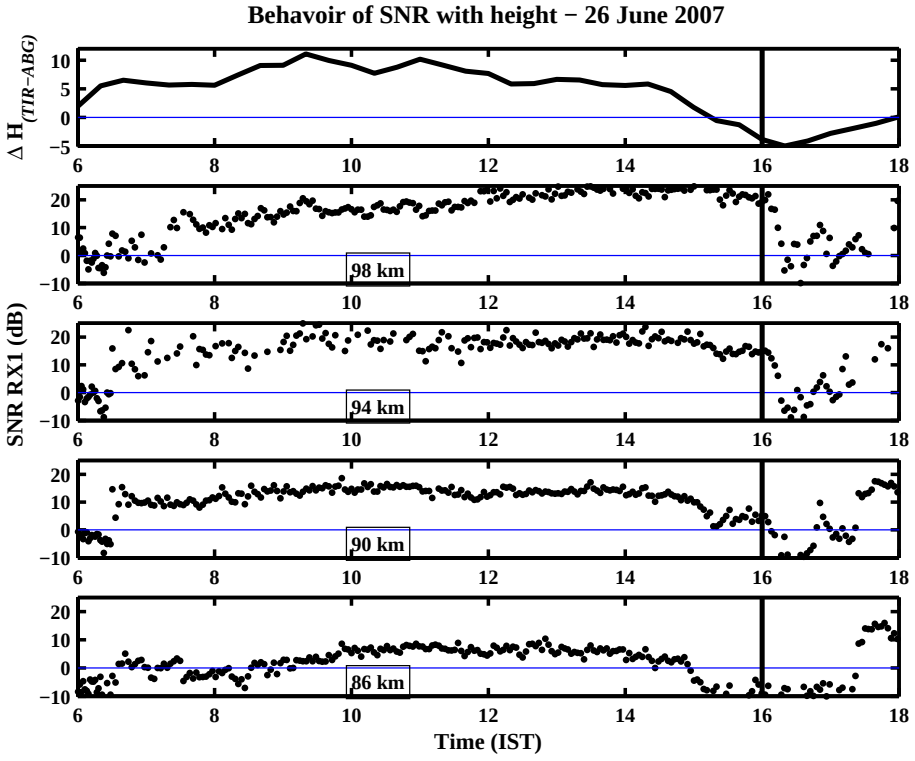

Fig. 2a. Temporal variation of electrojet strength (top panel) given by $[\Delta H_{\mathrm{TIR}} - \Delta H_{\mathrm{ABG}}]$ and SNR for 86, 90, 94, and 98 km on 26 June 2007 (four panels from the bottom).

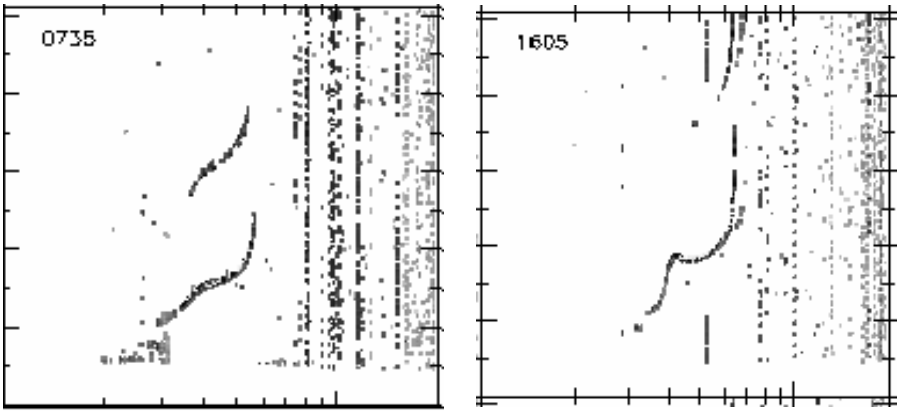

Fig. 2b. Ionograms recorded at 07:35 (left) and 16:05 IST (right) on 26 June 2007, showing various E_{sq} conditions. (left) Ionogram sample depicting the presence of E_{sq} and (2) (right) ionogram indicating the absence of E_{sq} trace.

the lower E-region heights. The pattern orientation can be seen strongly aligned in the north-south direction even at heights as low as 86 km during the times (10:00 to 15:00 IST) when the EEJ was strong. The axial ratio and the pattern scale do not appear to show any dependence on EEJ on this day, though in general these parameters were smaller at 94 and 98 km than those estimated for 86 and 90 km.

Whenever ΔH reverses, E_{sq} weakens as seen in the ionograms (sample is shown in Fig. 2b) and vanishes completely just before the time of CEJ maximum. Several of the SNR values in the lower E region heights fall below the threshold due to the absence of scatterers. The antenna parameters at these times could not be retrieved because of the rejection criterion (SNR<-6 dB) built in the analysis. The vertical line shown in Fig. 2a, c and d indicates the time (16:05 IST)

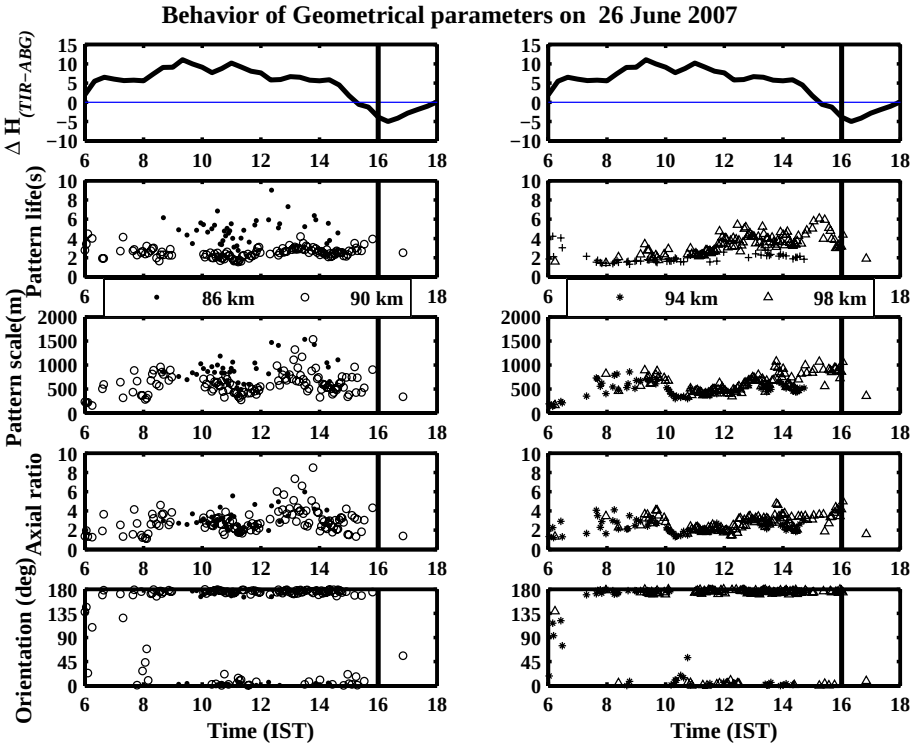

Fig. 2c. $[\Delta H_{\mathrm{TIR}} - \Delta H_{\mathrm{ABG}}]$ (top panels) and temporal variation of various geometrical parameters for 86, 90, 94 and 98 km (remaining panels) on 26 June 2007. See text for more details.

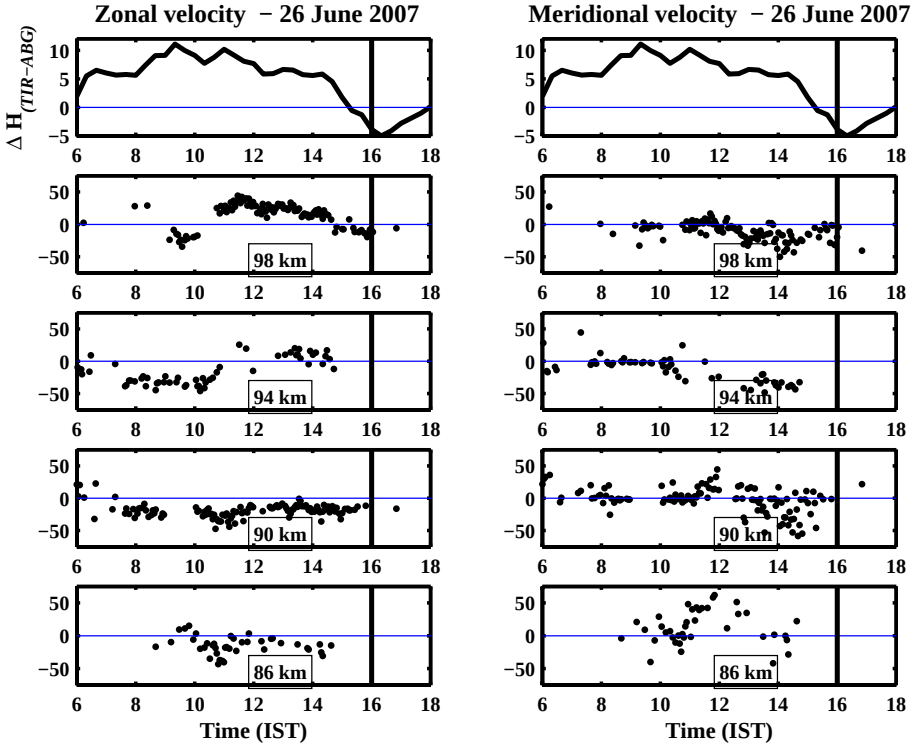

Fig. 2d. $[\Delta H_{\mathrm{TIR}} - \Delta H_{\mathrm{ABG}}]$ (top panels) and zonal and meridional velocities at 86, 90, 94 and 98 km (remaining panels) on 26 June 2007. See text for more details.

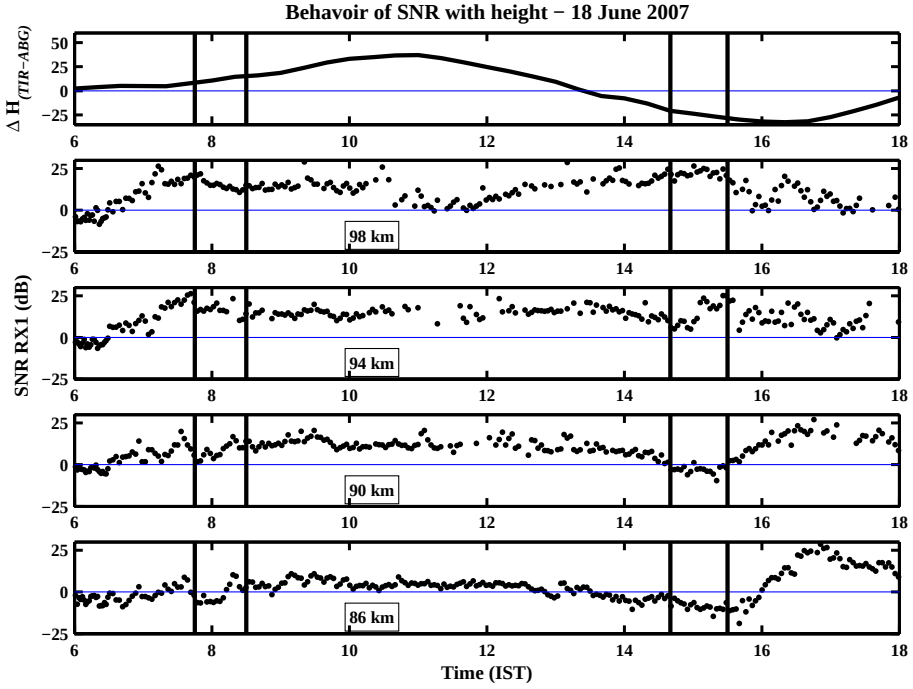

Fig. 3a. Same as Fig. 2a but for 18 June 2007.

at which E_{sq} disappeared in the ionograms. No useful data could be retrieved after 16:05 IST (except for one point as seen in Fig. 2c and d) and till 18:30 IST, because of low SNR throughout this time interval. When the error codes were examined, it was found the error code 10, that corresponds to the criterion that the apparent velocity is ten times greater than the true velocity, had contributed to the rejection of several data points at heights above 90 km in the morning hours (between 08:00 and 10:00 IST) when the E_{sq} was strong, and error code 2 (SNR<-6 dB) had contributed to the rejection of data in the afternoon hours (after 16:00 IST) when the E_{sq} was not seen in the ionograms.

The zonal velocities shown in Fig. 2d revealed a transition from westward to eastward flow at 11:00 IST at 94 and 98 km, while they remained mostly westward at 86 and 90 km. The meridional velocities were smaller in magnitude (around zero speed) in the morning hours at 94 and 98 km. They tend to attain larger values immediately after noon. Like pattern scale size and axial ratio, both zonal and meridional velocities in the lower E-region heights do not show any apparent dependence on the EEJ variation on this day.

Case-II: Quiet day marked with occurrence of strong E_{sb} (18 June 2007 (A_p=5) (Fig. 3a–d))

The top panels of Fig. 3a, c and d show $[\Delta H_{\mathrm{TIR}}-\Delta H_{\mathrm{ABG}}]$ representing the daytime electrojet strength. This is a good example for a CEJ day marked by a characteristic increase in electrojet strength in the morning hours followed by an afternoon strong depression in ΔH (peak negative value of $\sim$30 nT). The CEJ occurred from 13:15 IST to 18:15 IST. The sample ionograms shown in Fig. 3b were obtained at times 07:55 IST and 14:55 IST. The ionogram at 07:55 IST reveals strong E_{sq}, whereas the one at 14:55 IST shows the presence of blanketing E_s layer.

The increase in SNR in the morning hours (between 06:00 and 08:00 IST) prominently seen at heights 94 and 98 km (refer to Fig. 3a), occurred during the development of strong E_{sq} as observed in the ionograms. The duration over which strong E_{sq} appeared in the ionograms is indicated by the vertical lines in Fig. 3a, c and d. It may be noted that the morning E_{sq} observed at this time was stronger by 10–15 dB than at similar times on 26 June 2007. The SNR after reaching a peak at 08:00 IST appears to level off at 94 and 98 km. At lower heights, the SNR decreased for a brief duration at around 07:30 IST and later recovered. The E_{sq} intensity reduced to a moderate level at 08:30 IST and remained at this level till its disappearance in the afternoon hours. With regard to the geometrical parameters depicted in Fig. 3c, the pattern lifetimes initially increased prior to 08:00 IST and later attained smaller ($\sim$2 s) values. The longer pattern lifetimes in the morning hours are probably due to specular reflectors associated with strong E_{sq} occurrence. The pattern scales were mostly in the range 300–400 m and the axial ratio was between 2 and 3. Both these latter parameters were smaller on this day than on 26 June 2007. Interestingly, the pattern orientation seems to deviate away from its preferred north-south direction when the E_{sq} was strong in the morning hours.

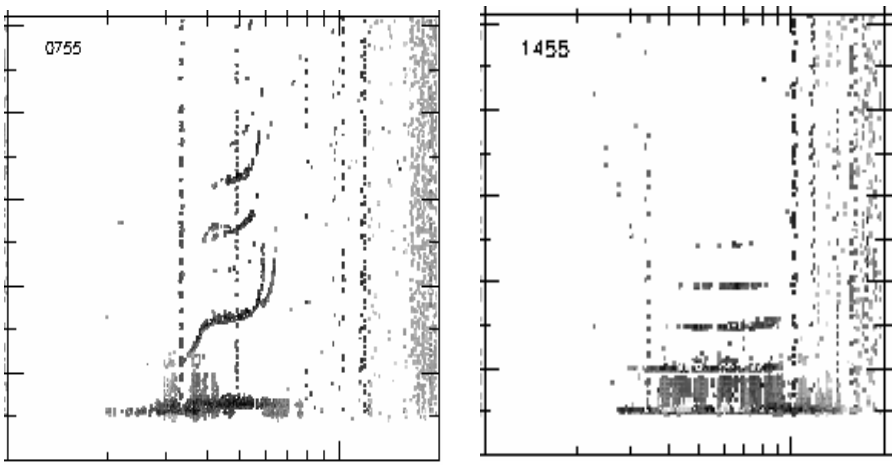

Fig. 3b. Ionograms recorded at 07:35 (left) and 14:55 IST (right) on 18 June 2007. **(1)** Sample ionogram showing the presence of strong E_{sq} (left). **(2)** Sample ionogram revealing the presence of blanketing E_s (right).

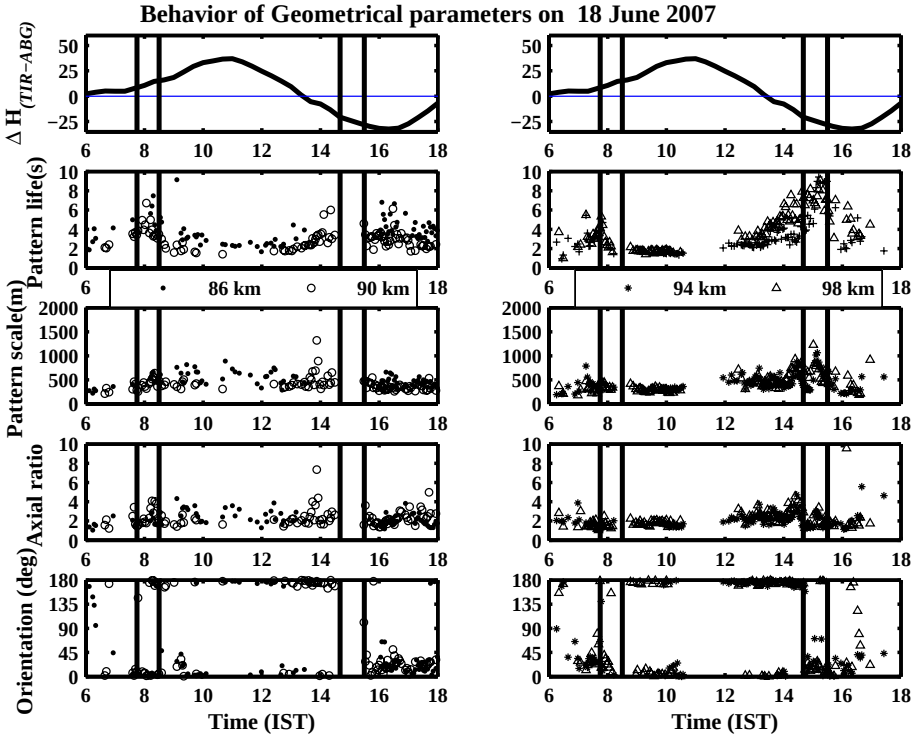

Fig. 3c. Same as Fig. 2c but for 18 June 2007.

In contrast to the observations on 26 June 2007, the E_{sq} on 18 June 2007 began to weaken at 14:00 IST and a blanketing E_s appeared at 14:40 IST. The E_{sb} event lasted till 15:25 IST. The appearance and disappearance of E_{sb} are indicated in the form of vertical lines in Fig. 3a, c and d. The SNR reveals distinct height dependence in the afternoon hours when the blanketing E_s was in progress. While the SNR at 98 km increased between 14:00 and 15:00 IST and later decreased to reach a minimum at 16:00 IST, at lower heights (86 and 90 km) the SNR rather decreased to reach a minimum between 15:00 and 16:00 IST and later increased. At the time of blanketing, the echo intensities were distinctly different between the two height regions. The smaller SNR at lower heights contributed to the rejection of data during this period. Interestingly, the SNR started increasing at around 15:00 IST at 90 km and about 30 min later at 86 km to reach large values (>20 dB) at 17:00 IST. Referring to Fig. 1, it may be noted that there was an anomalous rise in the echo intensity at

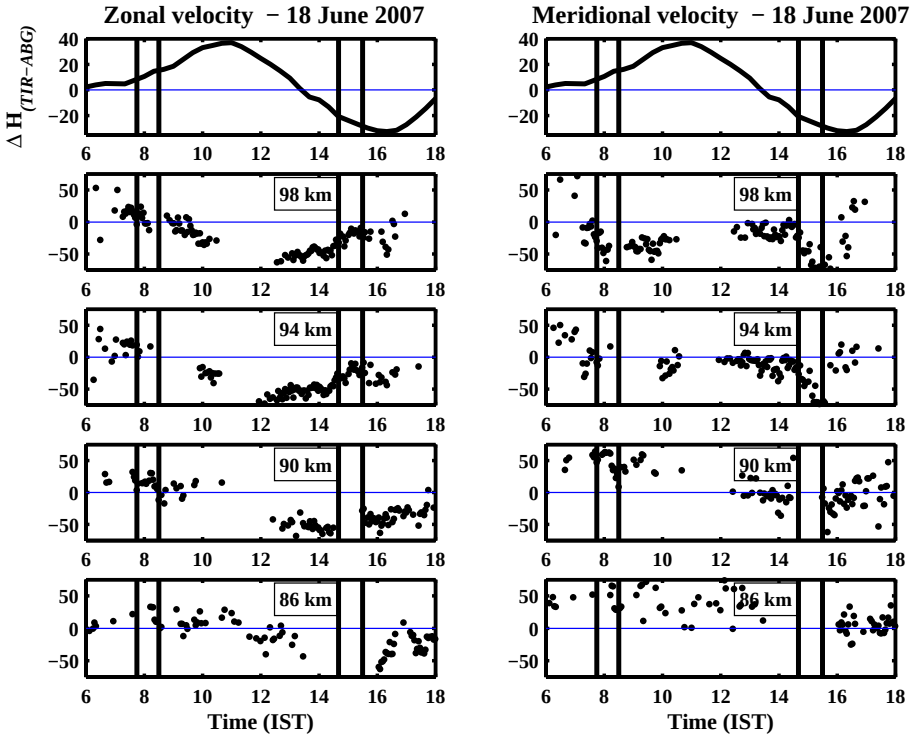

Fig. 3d. Same as Fig. 2d but for 18 June 2007.

intermediate heights (84–90 km) immediately after the blanketing E_s layer event. It is not known whether this anomalous enhancement in SNR is related to the blanketing event.

Previous studies reported on the behavior of SNR and geometrical parameters during the afternoon hours on CEJ days, wherein the geometrical parameters were shown to deviate from the expected behaviour (shorter pattern lifetimes, pattern elongation along north-south direction and low SNR values), soon after ΔH reversed and the electric field control was lost (Ramkumar et al., 2002; Gurubaran et al., 2007).

In the present scenario with information available on the occurrence of blanketing E_s, we observe an increase in SNR, high pattern life time and randomization of pattern orientation at 98 km in the afternoon hours when E_{sb} occurred. The SNR continued to remain high at 98 km alone, whereas the lower heights of 90 km and 94 km were marked by a drop in SNR, followed by a rise around 16:00 IST after the disappearance of blanketing E_s as mentioned earlier. The observations on this day provide evidence for the presence of height dependent scattering regions below the electrojet when probed by the MF radar.

The daytime zonal velocities at 96 and 98 km depicted in Fig. 3d clearly follow the ΔH curve with largest westward drift motions observed when ΔH was at its maximum. Data gaps between 11:00 and 12:30 IST at these heights were primarily due to signal saturation that the analysis takes into account and the corresponding data points are rejected. When the CEJ was in progress accompanied by blanketing E_s, the zonal drifts had decelerated, but interestingly large equatorward velocities were observed around this period. The meridional drift speeds at the highest altitude sampled by the radar exceeded 75 m/s at 16:00 IST when E_{sb} was about to disappear in the ionograms. The equatorward motions later decelerated and turned poleward at 16:30 IST.

4 Discussion

The MF radar at Tirunelveli operates close to the magnetic equator, wherein the electric fields associated with the equatorial electrojet control the electron drifts and also drive the two kinds of plasma instabilities, namely, the two-stream and gradient drift instabilities. Past VHF radar observations have categorized the radar echoes as Type I and Type II, primarily in terms of the irregularities these instabilities produce. These irregularities have distinct Doppler spectral signatures. It is also well established that the normal daytime E_{sq} as seen in the ionograms is caused by the gradient drift instability mechanism (Rastogi, 1972; Balsley et al., 1976). When the normal eastward electric field reverses as occurs during a counterelectrojet event, the Type II echoes recorded by VHF radars disappear, and the Esq disappears as well in the ionograms (Rastogi, 1973; Fejer et al., 1976).

The blanketing sporadic E as observed by the ionosonde is characterized by several multiple reflections and sometimes

almost totally blanketing the F layer. In a recent work, Devasia et al. (2004) used VHF radar observations from Trivandrum and demarcated the characteristics of Type II echoes due to E_{sq} and E_{sb} during CEJ events in terms of their height of occurrence, signal strength and associated Doppler spectral characteristics. An important observational feature reported in this study is the explosive and extremely variable nature of the VHF radar echoes during an E_{sb} event that were associated with small zonal drifts and significant distortions in the height profile of the drift velocity of the Type II irregularities. The radar echoes and the spectral features observed during the strong E_{sb} event were attributed to the sharp density gradient present in the intense E_{sb} layers that would provide favourable conditions for the growth of the instability even though the zonal drifts were small. The presence of height-varying Doppler velocities was suggested to be due to the modulation of electrojet current by the electric fields generated by height-varying winds with large shears.

MF radars are potential tools to probe the mesosphere-lower thermosphere region as they provide continuous wind measurements at a time resolution of typically two minutes. The MF radar observations made at Tirunelveli have posed problems in interpreting the drift measurements in terms of winds in the probing region 94–98 km (Ramkumar et al., 2002). Because the variation in the drift velocities, especially in the zonal component, often correlates well with ΔH, the measured zonal drifts at these heights are expected to be dominated by the electric field that drives the EEJ. It is puzzling that there are several occasions when the zonal velocities are eastward that cannot be attributed to the electric field drive alone (Ramkumar et al., 2002; Gurubaran et al., 2007). During normal EEJ conditions and at EEJ heights, the vertical electric field is upward and drives the EEJ producing the westward electron drift motion. Whether the ambient vertical electric field is downward directed at certain times that can drive an eastward drift at the radar probing heights is yet to be ascertained.

Making use of the co-located digital ionosonde, the present work aims at understanding the characteristics of the MF radar echoes and it has become possible to categorize the echoes and relate them to the specific ionospheric conditions noted in the ionosonde records. Two magnetically quiet days were selected and on each of these days an afternoon CEJ occurred. On one day (26 June 2007) the E_{sq} echoes disappeared in the afternoon hours, whereas on the other day (18 June 2007) the E_{sq} was replaced by an intense E_{sb} event. Additionally, during the morning hours on 18 June 2007, the E_{sq} was stronger by 10–15 dB than at similar times on the other day.

The increase in SNR in the lower E-region heights during the morning hours and its weakening when the CEJ was in progress in the afternoon hours could be clearly related to the appearance and disappearance of E_{sq} as seen in the ionograms. Because E_{sq} itself is believed to be a manifestation of Type II echoes (Balsley et al., 1976), we may argue that the scatterers that are responsible for the MF radar echoes are largely driven by the same plasma instability process that causes the Type II echoes for VHF radar and produces E_{sq} observed by the ionosonde. The full correlation analysis determines shorter pattern lifetimes ($\sim$2 s) during such conditions clearly indicating the unstable nature of the scattering medium. A remarkable feature noticed during the afternoon hours on 26 June 2007 is the weakening of SNR by 20–30 dB at 94 and 98 km that led to the rejection of useful data points due to poor SNR criterion. The disappearance of E_{sq} and the southward deflection of the horizontal component of the geomagnetic field at Tirunelveli confirm that the primary electric field had reversed and had not provided favourable conditions for the gradient drift instability mechanism to operate. Previous observations by Chandra and Rastogi (1973) that made use of HF spaced receiver records from Thumba reported fast fading, westward drift, highly elongated pattern due to preferential orientation in the N-S direction with a small semi-minor axis when E_{sq} was present. When E_{sq} disappeared in the ionograms, it was noticed that fadings were slow, the drift was eastward and the ground diffraction pattern was almost isotropic.

The MF radar observations during the afternoon hours on 18 June 2007 were made when a blanketing E_s event was in progress. As soon as ΔH reversed, the E_{sq} disappeared in the ionograms and was quickly replaced by the E_{sb} layer with its characteristic multiple reflection traces. The E_{sb} event lasted for about 50 min. The MF radar echoes revealed very distinct height behaviour during the afternoon hours on this day. The SNR at 86 and 90 km reveals gradual reduction in its values as ΔH was approaching its minimum at 16:00 IST. On the other hand the SNR at 98 km clearly reveals a rising trend resulting in a peak that coincided with the appearance of blanketing E_s in the ionograms. When compared to the explosive nature of the VHF radar echoes reported by Devasia et al. (2004), the MF radar echoes appear to have responded differently to the E_{sb} event, as they neither had the sharp buildup nor undergo random variations like the VHF radar echoes. It may also be noted that the contours shown in Fig. 1 reveal a descent of the enhanced echo intensities from 98 km to heights as low as 84 km. The anomalous enhancement in SNR at 86 km immediately after the blanketing E_s event is a puzzling observational feature reported in this work.

The drift velocities in the zonal and meridional directions determined from the full correlation analysis were also examined in this work. The geomagnetic activity index was very quiet (A_p=3) on 26 June 2007 and the EEJ did not develop then (largest value was $\sim$10 nT). On 18 June 2007, A_p was only 5 and the EEJ was intense with a peak value of $\sim$35 nT. Based on the electrojet strength, one may anticipate that the drift speeds at the highest height probed by the MF radar would be more westward on 18 June 2007 than on 26 June 2007. Though observations on 18 June 2007 revealed westward drift motions at 98 km with speeds exceeding 50 m/s,

the motion field was eastward directed with greatest speeds in the range 40–50 m/s on 26 June 2007. As heights decreased, the eastward motions turned westward on the weak EEJ day. This observation is baffling to the authors and it cannot be ascertained at this stage whether the motions detected at 98 km on 26 June 2007 represent neutral wind or a component of electron drift driven by an oppositely directed electric field.

Using the VHF radar data from Pohnpei, Tsunoda and Ecklund (1999) reported a counterstreaming westward current region at 93 km below the normal eastward electrojet. Because normal echoes could not be sustained by the gradient drift instability driven by a westward electric field, it was inferred then that the same gradient drift instability could act on potential large-scale plasma density structures driven by neutral turbulence leading to Type II echoes, even when the electrons were streaming eastward below the base of the EEJ region. The MF radar observations on 26 June 2007 present a case for an eastward drifting or counterstreaming region in the height region 94–98 km that needs to be explored further.

We next analyze the results on drift velocities derived from the full correlation analysis during the E_{sb} event on 18 June 2007. Earlier, Chandra and Rastogi (1975) examined the results from their ionospheric drift experiments performed at Kodaikanal (10.0° N, 77.5° E) during blanketing E_s events. Noting that E_{sb} preferentially occurred during the period of a very weak or reversed electrojet current, this study found predominantly eastward drift component during the absence of E_s and large north-south component of drift when E_{sb} was present. Over Tirunelveli, though the zonal velocities were small when the E_{sb} was in progress, the meridional velocities between 94 and 98 km were large. Equatorward drift speeds of more than 75 m/s were observed just when the blanketing E_s was about to disappear in the ionograms. Chandra and Rastogi (1975) proposed a mechanism that considered the movement of ionization layers from higher latitudes to the magnetic equator due to a horizontal wind with a significant meridional component. In this mechanism, an E_s layer was to be formed at dip latitudes greater than 3° possibly by wind shear mechanism and a north-south drift of 50–100 m/s could transport this layer to the magnetic equator in less than its lifetime. It is not certain in our work that the large meridional drifts observed by the MF radar at the time of the afternoon E_{sb} event on 18 June 2007 do represent neutral winds.

With regard to the nature of the MF radar scatterers during the strong morning E_{sq} and afternoon E_{sb} conditions noticed on 18 June 2007, the larger pattern lifetimes (4-6 s) observed at these times imply that the scatterers were more stable and the strong radar echoes have possibly resulted from a specular reflection of transmitted waves from those scatterers. On the other hand, smaller pattern lifetimes ($\sim$2 s) observed at other times on this day, when the EEJ was strong, clearly indicate that the scattering medium was turbulent and the scatterers remained close to being isotropic.

5 Conclusion

MF radar observations made from Tirunelveli on two counter electrojet days during the summer of 2007 were presented in this work and the nature of the scatterers in response to different electrodynamical conditions that prevailed on these days was investigated. Availability of ionograms obtained from the co-located digital ionosonde has provided additional insights into the electric field control of the radar scatterers. In particular, the MF radar echo characteristics at lower E-region heights depend strongly on the ambient electrodynamical conditions and could be related to the appearance and disappearance of normal E_{sq}, strong E_{sq} and blanketing E_s, as observed in the ionosonde records. Some intriguing results like descending SNR features, anomalous enhancement in echo intensity at 86 km and large meridional drifts, all observed during the occurrence of blanketing E_s and eastward drifts in the height region 94–98 km noticed during the weak EEJ day, call for further investigation of the link between the MF radar scattering process and equatorial E-region electrodynamics.

Acknowledgements. The MF radar, the digital ionosonde and the magnetometer setup at Tirunelveli are operated and maintained by the Indian Institute of Geomagnetism with financial support from the Department of Science and Technology, Government of India. Technical support by K. Unnikrishnan Nair and C. Selvaraj is duly acknowledged. One of the authors (R. Dhanya) thanks the Director, Indian Institute of Geomagnetism, for offering a research scholarship.

Topical Editor U.-P. Hoppe thanks M. Kelley and another anonymous referee for their help in evaluating this paper.

References

Abdu, M. A., Denardini, C. M., Sobral, J. H. A., Batista, I. S., Muralikrishna, P., and de Paula, E. R.: Equatorial electrojet irregularities investigations using a 50 MHz back-scatter radar and a digisonde at Sao Luis: Some initial results, J. Atmos. Solar-Terr. Phys., 64, 1425–1434, 2002.

Balsley, B. B., Rey, A., and Woodman, R. F.: On the plasma instability mechanisms responsible for *Esq*, J. Geophys. Res., 81, 1391–1396, 1976.

Briggs, B. H.: The analysis of spaced sensor records by correlation techniques, Handbook for MAP., 13, 166–186, 1984.

Chandra, H. and Rastogi, R. G.: Some characteristics of the ionospheric irregularities associated with E_{sq} layers, J. Geophys. Res., 78, 3007–3012, 1973.

Chandra, H. and Rastogi, R. G.: Diffuse type and blanketing type sporadic E layer at Kodaikanal, Curr. Sci., 43, 533–535, 1974.

Chandra, H. and Rastogi, R. G.: Blanketing sporadic E layer near the magnetic equator, J. Geophys. Res., 80, 149–153, 1975.

Crochet, M., Hanuise, C., and Broche, P.: HF radar studies of two-stream instability during an equatorial counter electrojet, J. Geophys. Res., 84, 5223–5233, 1979.

Devasia, C. V., Jyoti, N., Subbarao, K. S. V., Diwakar Tiwari, and Raghava Reddi, C.: On the role of vertical elec-

tron density gradients in the generation of type II irregularities associated with blanketing E_s (E_{sb}) during counter equatorial electrojet events: A case study, Radio Sci., 39, RS3007, doi:10.1029/2002RS002725, 2004.

Farley, D. T.: A plasma instability resulting in field aligned irregularities in the ionosphere, J. Geophys. Res., 68, 6083–6097, 1963.

Farley, D. T. and Balsley, B. B.: Instabilities in the equatorial electrojet, J. Geophys. Res., 78, 227–239, 1973.

Fejer, B. J., Farley, D. T., Balsley, B. B., and Woodman, R. F.: Vertical structure of the VHF backscattering region in the equatorial electrojet and the gradient drift instability, J. Geophys. Res., 80, 1313–1324, 1975.

Fejer, B. J., Farley, D. T., Balsley, B. B., and Woodman, R. F.: Radar studies of anomalous velocity reversals in the equatorial ionosphere, J. Geophys. Res., 81, 4621–4626, 1976.

Gurubaran, S. and Rajaram, R.: Signatures of equatorial electrojet in the mesospheric partial reflection drifts over magnetic equator, Geophys. Res. Lett., 27, 943–946, 2000.

Gurubaran, S., Dhanya, R., Sathishkumar, S., and Paramasivan, B.: On the electric field control of the MF radar scatterers in the lower E region over the magnetic equator, Geophys. Res. Lett., 34, L06105, doi:10.1029/2006GL028748, 2007.

Kelley, M. C.: The Earth's ionosphere: Plasma physics and electrodynamics, Academic Press, 1989.

Lesicar, D.: Study of the structure of partial reflection radar scatterers and their application in atmospheric applications, Ph.D. Thesis, The University of Adelaide, 1993.

Ramkumar, T. K., Gurubaran, S., and Rajaram, R.: Lower E-region MF radar spaced antenna measurements over magnetic equator, J. Atmos. Solar-Terr. Phys., 64, 1445–1453, 2002.

Rastogi, R. G.: Sudden disappearance of E_{sq} and the reversal of the equatorial electric fields, Ann. Geophys., 28, 717–728, 1972, http://www.ann-geophys.net/28/717/1972/.

Rastogi, R. G.: Equatorial sporadic E and the electric field, J. Atmos. Terr. Phys., 35, 367–371, 1973.

Reddy, C. A., Vikramkumar, B. T., and Viswanathan, K. S.: Electric fields in the equatorial ionosphere: A review of techniques and measurements, J. Atmos. Terr. Phys., 49, 183–191, 1987.

Tabbagh, J., Carter, D. A., Balsley, B. B., Broche, P., and Crochet, M.: Irregularity drift velocities in the equatorial electrojet observed by both the close-spaced antenna technique and the Doppler radar method, J. Atmos. Terr. Phys., 39, 1035–1039, 1977.

Tsunoda, R. T. and Ecklund, W. L.: On the nature of radar echoes below 95 km during counter streaming in the equatorial electrojet, Geophys. Res. Lett., 26, 2717–2720, 1999.

Vincent, R. A.: Gravity wave motions in the mesosphere, J. Atmos. Terr. Phys., 46, 119–128, 1984.